

IMECE2002-PVP-32292

COMPUTATIONAL METHODS FOR THE DESIGN OF DEFORMATION PROCESSES OF POROUS MATERIALS

Nicholas Zabaras and Shankar Ganapathysubramanian
Materials Process Design and Control Laboratory
Sibley School of Mechanical and Aerospace Engineering
188 Frank H. T. Rhodes Hall
Cornell University
Ithaca, NY 14853-3801
Email: zabaras@cornell.edu

ABSTRACT

An updated Lagrangian framework of the continuum sensitivity method (CSM) is presented to address important computational design problems in the deformation processing of porous materials. Weak sensitivity equations are developed that are consistent with the kinematic, constitutive, contact and thermal analyses used in the solution of the direct thermomechanical problem. The CSM is here used to analyze die and preform computational design problems in industrial metal forming processes wherein temperature and the accumulated damage play an important role in influencing the deformation mechanism, material state and shape of the deformed workpiece.

INTRODUCTION

We are herein interested in the development of a continuum sensitivity method that addresses the design of forming processes for porous materials so as to meet specific industrial requirements. The Gurson-Tvergaard-Needleman model is widely used in literature and will be employed in this work as well (Gurson, 1977).

Continuum damage mechanics was used earlier in the design of forming processes of porous materials (Picart et al., 1977). This work involves the design of a preform for H-shaped axisymmetric forging. In Picart et al. (1998), a gradient-based optimization approach was introduced using sensitivities obtained through the direct differentiation method (DDM), which is significantly different from the continuum sensitivity method (CSM) which is the focus of

our paper. A more recent effort includes the work in Chung et al. (2000) where an optimal process design methodology was presented using a flow formulation. Relative density is used as the state variable unlike in our effort, where void fraction is defined as one of the state variables. A direct differentiation scheme is used to evaluate the sensitivities. This is achieved by differentiating the numerical counterparts of the continuum equations. The stiffness matrix in the FEM solution of the sensitivity problem was also approximated through a finite difference scheme. Our effort markedly differs from these approaches in that, we first design-differentiate the continuum laws and then discretize the obtained continuum sensitivity equations.

In our earlier work, we developed a Lagrangian analysis for modeling of metal forming operations for materials with ductile damage (Srikanth and Zabaras, 1999). Most of our effort towards the development of computational design algorithms for forming processes was restricted to materials with no damage evolution. These efforts are summarized in References [6-9] where the CSM is used as the main design tool for the evaluation of sensitivities. Preform, die and other process parameter design problems were discussed and the CSM-based sensitivity fields were used to obtain the gradient of appropriately defined cost functional and constraints. This paper extends our earlier work and presents the development of a continuum sensitivity method for the calculation of sensitivity fields for non-steady thermomechanical forming processes for materials with ductile

damage. Some preliminary die and preform design examples are also presented.

DIRECT PROBLEM ANALYSIS

Consider \mathcal{B}_0 as the initial configuration of the body ($t = 0$) and \mathcal{B}_{n+1} as the current configuration ($t = t_{n+1}$). The reference configuration in an updated Lagrangian formulation is taken as \mathcal{B}_n . Let \mathbf{X} be a material particle in \mathcal{B}_0 and $\mathbf{x} = \tilde{\mathbf{x}}(\mathbf{X}, t) \equiv \hat{\mathbf{x}}(\mathbf{x}_n, t)$ its location at time $t \in [t_n, t_{n+1}]$. The total deformation gradient, \mathbf{F}_{n+1} , is then defined in terms of the relative deformation gradient, \mathbf{F}_r , as follows:

$$\mathbf{F}_{n+1} = \nabla_n \tilde{\mathbf{x}}(\mathbf{x}_n, t_{n+1}) \nabla_0 \tilde{\mathbf{x}}(\mathbf{X}, t_n) = \mathbf{F}_r \mathbf{F}_n \quad (1)$$

In an appropriate kinematic framework for large deformation inelastic analysis including thermal effects, the total deformation gradient \mathbf{F} is decomposed as $\mathbf{F} = \mathbf{F}^e \mathbf{F}^p \mathbf{F}^\theta$, where \mathbf{F}^e is the elastic deformation gradient, \mathbf{F}^p , the plastic deformation gradient and \mathbf{F}^θ is the thermal part of the deformation gradient. Assuming isotropic thermal expansion, the evolution of \mathbf{F}^θ is given $\dot{\mathbf{F}}^\theta \mathbf{F}^{\theta^{-1}} = \beta \dot{\theta} \mathbf{I}$, where β is the thermal expansion coefficient, treated as a constant in this work, and \mathbf{I} is the second-order identity tensor. Finally, $\det \mathbf{F}^p = \frac{1-f_o}{1-f}$ is here taken as a measure of internal damage, where f_o and f represent the void volume fractions in the initial and deformed configurations, respectively.

The hyperelastic constitutive equations are written as follows,

$$\bar{\mathbf{T}} = \mathcal{L}^e [\bar{\mathbf{E}}^e] \quad (2)$$

where the strain measure, $\bar{\mathbf{E}}^e$, is defined with respect to the intermediate (unstressed) configuration as $\bar{\mathbf{E}}^e = \ln \mathbf{U}^e$. The corresponding conjugate stress measure $\bar{\mathbf{T}}$ is the pullback of the Kirchhoff stress with respect to \mathbf{R}^e ,

$$\bar{\mathbf{T}} = \det(\mathbf{U}^e) \mathbf{R}^{eT} \mathbf{T} \mathbf{R}^e \quad (3)$$

Here \mathbf{U}^e and \mathbf{R}^e are calculated from the polar decomposition, $\mathbf{F}^e = \mathbf{R}^e \mathbf{U}^e$, of \mathbf{F}^e . For an isotropic material, the elastic moduli \mathcal{L}^e are given by

$$\mathcal{L}^e = 2\mu \mathcal{I} + \left\{ \kappa - \frac{2}{3}\mu \right\} \mathbf{I} \otimes \mathbf{I} \quad (4)$$

where the shear modulus μ and bulk modulus κ are, in general, functions of f and θ (Zavaliangos and Anand (1992)

and Budiansky (1970)). Finally, \mathcal{I} denotes the fourth order identity tensor.

The equilibrium equation can be expressed on the reference configuration \mathcal{B}_n as,

$$\nabla_n \cdot \mathbf{P} + \mathbf{f} = \mathbf{0} \quad (5)$$

where $\nabla_n \cdot$ represents the divergence on the reference configuration and \mathbf{P} is the corresponding Piola-Kirchhoff I stress.

The deformation problem is solved incrementally in time starting from the given initial configuration \mathcal{B}_0 .

It is well known that the equivalent tensile stress σ_m of the matrix material should be defined implicitly in terms of the Cauchy stress \mathbf{T} and the void fraction f (Gurson, 1977). With the assumption of isotropy, a particular form of this dependence is as follows:

$$\Phi = \Phi(\sigma_m, f, p, \mathcal{S}) = 0 \quad (6)$$

where this dependence of the potential Φ on the stress $\bar{\mathbf{T}}$ is restricted to its first and second invariants. Here, $\mathcal{S} = \sqrt{\bar{\mathbf{T}}' \cdot \bar{\mathbf{T}}'}$, the norm of the stress deviator, $\bar{\mathbf{T}}' = \bar{\mathbf{T}} + p \mathbf{I}$, is given by where p is the mean normal pressure, $p = -\text{tr} \bar{\mathbf{T}}/3$. In this work, Φ is taken as

$$\Phi = \frac{3}{2} \frac{\mathcal{S}^2}{\sigma_m^2} - 1 + 2q_1 f^* \cosh\left(\frac{3}{2} q_2 \frac{p}{\sigma_m}\right) - (q_1 f^*)^2 = 0 \quad (7)$$

with $q_1 = 1.5$ and $q_2 = 1.0$. The function $f^*(f)$ proposed to handle the loss in the load carrying capacity for void fractions greater than a critical value f_c , is taken from Tvergaard and Needleman (1991).

Two scalar state variables are considered here, one representing the isotropic material hardening behavior, denoted by s , and the other, the volume void fraction, f . The evolution of the plastic part of the deformation gradient \mathbf{F}^p is given by the normality rule,

$$\bar{\mathbf{D}}^p = \dot{\gamma} \partial_{\bar{\mathbf{T}}} \Phi = \dot{\gamma} \left[(\partial_{\mathcal{S}} \Phi) \mathbf{N} - \frac{1}{3} (\partial_p \Phi) \mathbf{I} \right] \quad (8)$$

where $\bar{\mathbf{L}}^p = \dot{\mathbf{F}}^p \mathbf{F}^{p-1}$ and $\mathbf{N} = \frac{\bar{\mathbf{T}}'}{\mathcal{S}}$ is the direction of the stress deviator. The spin in the intermediate, hot, unstressed, plastically deformed configuration is assumed to vanish (for isotropic materials).

The work equivalence relation, $\bar{\mathbf{T}} \cdot \bar{\mathbf{D}}^p = (1-f)\sigma_m \dot{\bar{\epsilon}}_m^p$, is used to evaluate $\dot{\gamma}$ in Equation (8) as:

$$\dot{\gamma} = \left[\frac{(1-f)\sigma_m}{\mathcal{S}\partial_{\mathcal{S}}\Phi + p\partial_p\Phi} \right] \dot{\bar{\epsilon}}_m^p \quad (9)$$

Note that the notation $\partial_{\mathcal{S}}$ and ∂_p in the equations above is introduced to denote partial derivatives of Φ with respect to \mathcal{S} and p , respectively.

The evolution of the equivalent tensile plastic strain $\bar{\epsilon}_m^p$ is specified via uniaxial experiments as

$$\dot{\bar{\epsilon}}_m^p = f(\sigma_m, s, \theta) \quad (10)$$

and the evolution of s takes the form,

$$\dot{s} = g(\sigma_m, s, \theta) = h(\sigma_m, s, \theta)\dot{\bar{\epsilon}}_m^p - \dot{r}(s, \theta) \quad (11)$$

where $\dot{r}(s, \theta)$ is the static recovery function.

The evolution equation of f is of the form:

$$\dot{f} = (1-f)\text{tr}(\bar{\mathbf{D}}^p) \quad (12)$$

The mechanical dissipation \mathcal{W}_{mech} is required in the energy equation and is specified as

$$\mathcal{W}_{mech} = \omega \bar{\mathbf{T}} \cdot \bar{\mathbf{D}}^p = \omega (1-f) \sigma_m \dot{\bar{\epsilon}}_m^p \quad (13)$$

where $\omega \in [0.85, 0.95]$.

Using a radial return algorithm, it was shown that within a time step, the solution of a system of five non-linear algebraic equations for five unknowns, namely $\sigma_m, f, p, s, \mathcal{S}$, is required (Srikanth and Zabarar, 1999). The solution for these scalar variables follows a Newton-Raphson procedure with line search. It also incorporates the constraints, $\sigma_m \geq \delta$ and $\mathcal{S} \geq \delta$, where δ is a predefined tolerance introduced in the numerical implementation. Other details on the implementation of the constitutive problem and algorithms for the kinematic and contact subproblems of the direct problem can be found in Srikanth and Zabarar (1999).

PARAMETER AND SHAPE SENSITIVITY ANALYSIS

Definition of shape and parameter sensitivities

In this section, we summarize the shape and parameter sensitivities of a Lagrangian field Ω in an updated Lagrangian (UL) framework. Specific information on shape

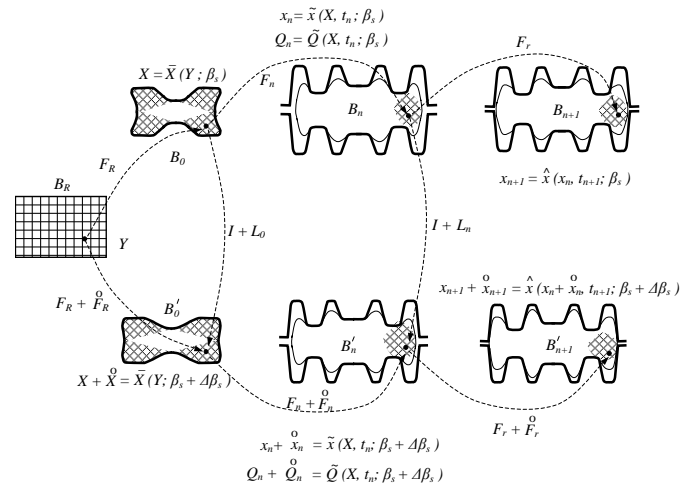


Figure 1. SCHEMATIC OF THE PROCEDURE USED TO COMPUTE THE SHAPE SENSITIVITIES IN THE TIME INCREMENT $[t_n, t_{n+1}]$ USING AN UL SENSITIVITY FORMULATION. \mathcal{B}_{n+1} REFERS TO THE CONFIGURATION THAT THE WORKPIECE OCCUPIES AT TIME $t = t_{n+1}$. FOR PARAMETER SENSITIVITY, THE REFERENCE CONFIGURATION \mathcal{B}_R , IS THE SAME AS THE INITIAL CONFIGURATION \mathcal{B}_0 and $\mathbf{F}_R = \mathbf{I}$.

and parameter sensitivities can be obtained from Badrinarayanan and Zabarar (1996), Srikanth and Zabarar (2000) and Ganapathysubramanian and Zabarar (2002).

Let us consider a generic field Ω that can represent \mathbf{x} , \mathbf{F}^e , s , f , T or any other material or deformation related field. Let β_p denote the design variables related to process conditions (such as the die surface, the ram speed or lubrication conditions), other than the preform surface. The dependence of the field $\Omega = \hat{\Omega}(\mathbf{x}_n, t)$ on β_p can be expressed as follows:

$$\Omega = \hat{\Omega}(\mathbf{x}_n, t; \beta_p) = \hat{\Omega}(\tilde{\mathbf{x}}(\mathbf{X}, t; \beta_p), t; \beta_p) = \tilde{\Omega}(\mathbf{X}, t; \beta_p) \quad (14)$$

where \mathbf{x}_n denotes the material point in the reference configuration corresponding to \mathbf{X} and \mathbf{x}_{n+1} in the initial and current configurations, respectively. The parameter sensitivity $\hat{\Omega} = \hat{\Omega}(\mathbf{x}_n, t; \beta_p, \Delta\beta_p)$ is defined as the total Gateaux differential of $\Omega = \hat{\Omega}(\mathbf{x}_n, t; \beta_p)$ in the direction $\Delta\beta_p$ computed at β_p

$$\hat{\Omega}(\mathbf{x}_n, t; \beta_p, \Delta\beta_p) = \left. \frac{d}{d\lambda} \tilde{\Omega}(\mathbf{X}, t; \beta_p + \lambda\Delta\beta_p) \right|_{\lambda=0} \quad (15)$$

For evaluating the shape sensitivities (sensitivities with respect to the preform shape), a design independent, reference material configuration \mathcal{B}_R is introduced and a smooth

bijjective, design dependent, geometric mapping defined on \mathcal{B}_R results in the various initial configurations (preforms) \mathcal{B}_0 (Fig. 1). Let β_s be the shape parameters that define the preform \mathcal{B}_0 or equivalently the mapping from \mathcal{B}_R to \mathcal{B}_0 . This geometric mapping is described as

$$\mathbf{X} = \bar{\mathbf{X}}(\mathbf{Y}; \beta_s) \quad \forall \mathbf{Y} \in \mathcal{B}_R \quad (16)$$

The dependence of the field $\Omega = \hat{\Omega}(\mathbf{x}_n, t)$ on β_s can be expressed as follows

$$\Omega = \hat{\Omega}(\mathbf{x}_n, t; \beta_s) = \tilde{\Omega}(\mathbf{X}, t; \beta_s) = \bar{\Omega}(\mathbf{Y}, t; \beta_s) \quad (17)$$

The shape sensitivity $\hat{\Omega} = \hat{\Omega}(\mathbf{x}_n, t; \beta_s, \Delta\beta_s)$ is then defined (in a similar fashion to the parameter sensitivities) as the total Gateaux differential (directional derivative) of $\Omega = \hat{\Omega}(\mathbf{x}_n, t; \beta_s)$ in the direction $\Delta\beta_s$ computed at β_s

$$\hat{\Omega}(\mathbf{x}_n, t; \beta_s, \Delta\beta_s) = \left. \frac{d}{d\lambda} \bar{\Omega}(\mathbf{Y}, t; \beta_s + \lambda\Delta\beta_s) \right|_{\lambda=0} \quad (18)$$

Figure 1 describes the computation of shape sensitivities in an updated Lagrangian framework. The descriptions of parameter and shape sensitivities (Equations (15) and (18)) are the same if the reference mapping \mathbf{F}_R for the parameter sensitivity problem was an identity map and in this case the velocity design gradient $\mathbf{L}_R = \overset{\circ}{\mathbf{F}}_R \mathbf{F}_R^{-1} \equiv \mathbf{0}$. In the remainder of this paper, the notation $\overset{\circ}{\cdot}$ is used, for convenience, to define both parameter and shape sensitivities.

Deformation sensitivity problem

The essential feature of the CSM is that equations governing the sensitivity fields are computed at the continuum level. The equilibrium equation is considered and ‘design differentiated’. This differential sensitivity equilibrium equation is then posed in a weak form so as to establish a principle of virtual work like equation for the calculation of the sensitivity of deformation fields (Ganapathysubramanian and Zabaras, 2002). Consistent with this mode of analysis, the sensitivity constitutive, sensitivity thermal and sensitivity contact equations are derived from their corresponding continuum equations rather than their numerically integrated counterparts.

For completeness, we briefly review the kinematic sensitivity problem. The deformation sensitivity problem is developed on the reference configuration \mathcal{B}_n . A variational form for the sensitivity equilibrium equation can be posed

as follows: Evaluate $\overset{\circ}{\mathbf{x}} = \hat{\mathbf{x}}(\mathbf{x}_n, t; \beta, \Delta\beta)$ such that

$$\int_{\mathcal{B}_n} \left[\overset{\circ}{\mathbf{P}} \cdot \nabla_n \tilde{\boldsymbol{\eta}} - \mathbf{P} \left[\nabla_n \cdot \mathbf{L}_n^T \right] \cdot \tilde{\boldsymbol{\eta}} - \left(\mathbf{P} \mathbf{L}_n^T \cdot \nabla_n \tilde{\boldsymbol{\eta}} \right) \right] dV_n = \int_{\partial\mathcal{B}_n} \left\{ \overset{\circ}{\boldsymbol{\lambda}} - [\mathbf{L}_n \cdot (\mathcal{N} \otimes \mathcal{N})] \boldsymbol{\lambda} \right\} \cdot \tilde{\boldsymbol{\eta}} dA_n \quad (19)$$

for every $\tilde{\boldsymbol{\eta}}$, where $\tilde{\boldsymbol{\eta}}$ is a kinematically admissible sensitivity deformation field expressed over the reference configuration \mathcal{B}_n . Also here, β is the design vector (can represent either β_p or β_s), $\Delta\beta$ represents a perturbation to the design vector, \mathcal{N} is the unit normal in $\partial\mathcal{B}_n$ and $\mathbf{L}_n \equiv \nabla_n \hat{\mathbf{x}}(\mathbf{x}_{n-1}, t_n; \beta, \Delta\beta) = \overset{\circ}{\mathbf{F}}_n \mathbf{F}_n^{-1}$ refers to the design velocity gradient. In the case of parameter sensitivity analysis, the design velocity gradient at time t_0 , $\mathbf{L}_0 = \mathbf{0}$. In the case of shape sensitivity analysis, the design velocity gradient at time t_0 , $\mathbf{L}_0 = \nabla_0 \bar{\mathbf{X}}(\mathbf{X}; \beta_s, \Delta\beta_s) = \mathbf{L}_R = \overset{\circ}{\mathbf{F}}_R \mathbf{F}_R^{-1}$ (see Fig. 1). As noted earlier, $\mathbf{L}_0 = \overset{\circ}{\mathbf{F}}_R$, since $\mathbf{F}_R = \mathbf{I}$ in this implementation.

We need the relationships between (a) $\overset{\circ}{\mathbf{F}}_r$ and $\overset{\circ}{\mathbf{x}}$ (b) $\overset{\circ}{\mathbf{P}}$ and $[\overset{\circ}{\mathbf{F}}_r, \overset{\circ}{\boldsymbol{\theta}}]$ and (c) $\overset{\circ}{\boldsymbol{\lambda}}$ and $\overset{\circ}{\mathbf{x}}$ to complete the variational sensitivity problem. The relationship between $\overset{\circ}{\mathbf{F}}_r$ and $\overset{\circ}{\mathbf{x}}$ is purely kinematic:

$$\overset{\circ}{\mathbf{F}}_r = \overline{\nabla_n \mathbf{x}} = \nabla_n \overset{\circ}{\mathbf{x}} - \mathbf{F}_r \mathbf{L}_n \quad (20)$$

The relationship between $\overset{\circ}{\mathbf{P}}$ and $[\overset{\circ}{\mathbf{F}}_r, \overset{\circ}{\boldsymbol{\theta}}]$ is obtained from the sensitivity constitutive problem to be discussed in the next section. It takes the following form:

$$\overset{\circ}{\mathbf{P}} = \mathcal{A} [\overset{\circ}{\mathbf{F}}_r] + \mathbf{B} \overset{\circ}{\boldsymbol{\theta}} + \mathbf{C} \quad (21)$$

where \mathcal{A} is a fourth order tensor and \mathbf{B} , \mathbf{C} are second order tensors. These tensors, are constants, defined from known direct and sensitivity fields at the previous time step. Also note that $\overset{\circ}{\mathbf{F}}_{n+1}$ is related to $\overset{\circ}{\mathbf{F}}_r$ as

$$\overset{\circ}{\mathbf{F}}_{n+1} = \overset{\circ}{\mathbf{F}}_r \mathbf{F}_n + \mathbf{F}_r \overset{\circ}{\mathbf{F}}_n \quad (22)$$

The above equation can be used to transform the linear relation of the sensitivity of any field with $\overset{\circ}{\mathbf{F}}_{n+1}$ to a linear relation with respect to $\overset{\circ}{\mathbf{F}}_r$.

The relationship between $\overset{\circ}{\boldsymbol{\lambda}}$ and $\overset{\circ}{\boldsymbol{x}}$ as needed in Equation (19) is obtained from the sensitivity contact problem as:

$$\overset{\circ}{\boldsymbol{\lambda}} = \boldsymbol{D} [\overset{\circ}{\boldsymbol{x}}] + \boldsymbol{d} \quad (23)$$

where \boldsymbol{D} is a second order tensor and \boldsymbol{d} a vector. The non-trivial derivation of these tensors resulting by design-differentiation of a regularized contact problem can be found in Zabaras et al. (2000).

Constitutive sensitivity sub-problem

The solution of the direct thermo-mechanical problem is known at time t_{n+1} i.e. the set $\{\boldsymbol{T}, s, f, \boldsymbol{F}^e\}$, the body configuration \mathcal{B}_{n+1} as well as the temperature field θ_{n+1} are known at t_{n+1} . The constitutive sensitivity problem is history dependent and the solution of the sensitivity problem at time t_n is assumed known, yielding the variables $\{\overset{\circ}{\boldsymbol{T}}, \overset{\circ}{s}, \overset{\circ}{f}, \overset{\circ}{\boldsymbol{F}}^e\}$ at the beginning of each time increment. In Ganapathysubramanian and Zabaras (2002), it was shown that the deformation sensitivity response is dependent only on the instantaneous temperature sensitivity response $\overset{\circ}{\theta}_{n+1}$ (for constant thermal expansion coefficient). We will here show that the integration of the evolution equations for the sensitivity of the plastic and thermal deformation gradients, the evolution equation for the sensitivity of the state variable s and the evolution equation for the sensitivity of the volume void fraction f will allow us to advance the solution of the sensitivity constitutive sub-problem. The relationship, between $\overset{\circ}{\boldsymbol{T}}$ and $[\overset{\circ}{\boldsymbol{F}}, \overset{\circ}{\theta}]$ at time t_{n+1} as given in Equation (21) will be computed. This relation is essential in the solution of the sensitivity thermo-mechanical problem (Equation (19)).

As part of the update procedure, one computes the set $\{\overset{\circ}{\boldsymbol{T}}, \overset{\circ}{s}, \overset{\circ}{f}, \overset{\circ}{\boldsymbol{F}}^e\}$ at the end of the time increment t_{n+1} where the sensitivity of the total deformation gradient $\overset{\circ}{\boldsymbol{F}}_{n+1}$ and the sensitivity of the temperature field $\overset{\circ}{\theta}_{n+1}$ are assumed known. The sensitivity $\overset{\circ}{\mathcal{W}}_{mech}$ of the mechanical dissipation \mathcal{W}_{mech} is also computed as being a driving force for the thermal sensitivity problem at time t_{n+1} .

Linear relation between $\overset{\circ}{\boldsymbol{F}}_{n+1}^p$ and $[\overset{\circ}{\boldsymbol{F}}_{n+1}^e, \overset{\circ}{\theta}_{n+1}]$: The evolution equation for $\overset{\circ}{\boldsymbol{F}}^p$ is evaluated as follows:

$$\frac{\partial \overset{\circ}{\boldsymbol{F}}^p}{\partial t} = \bar{\boldsymbol{D}}^p \overset{\circ}{\boldsymbol{F}}^p + \bar{\boldsymbol{D}}^p \boldsymbol{F}^p \quad (24)$$

$\bar{\boldsymbol{D}}^p$ can be computed by design-differentiation of the flow rule (Equation (8)) as,

$$\bar{\boldsymbol{D}}^p = \overline{(\dot{\gamma} \partial_{\boldsymbol{T}} \Phi)} = \dot{\gamma} \left[(\partial_S \Phi) \boldsymbol{N} - \frac{1}{3} (\partial_p \Phi) \boldsymbol{I} \right] \quad (25)$$

which can be written as follows:

$$\bar{\boldsymbol{D}}^p = \boldsymbol{D}_1 \overset{\circ}{\sigma}_m + \boldsymbol{D}_2 \overset{\circ}{f} + \boldsymbol{D}_3 \overset{\circ}{p} + \boldsymbol{D}_4 \overset{\circ}{S} + \boldsymbol{D}_5 \overset{\circ}{s} + \boldsymbol{D}_6 \overset{\circ}{\theta} + d_7 \overset{\circ}{\boldsymbol{T}}' \quad (26)$$

where $\boldsymbol{D}_1, \boldsymbol{D}_2, \boldsymbol{D}_3, \boldsymbol{D}_4, \boldsymbol{D}_5, \boldsymbol{D}_6$ are known second order tensors and d_7 a known scalar as given below:

$$\boldsymbol{D}_1 = \frac{\dot{\gamma} \overset{\circ}{\sigma}_m}{\dot{\gamma}} \bar{\boldsymbol{D}}^p + \dot{\gamma} \left\{ \Phi_{S \sigma_m} \boldsymbol{N} - \frac{1}{3} \Phi_{p \sigma_m} \boldsymbol{I} \right\} \quad (27)$$

$$\boldsymbol{D}_2 = \frac{\dot{\gamma} \overset{\circ}{f}}{\dot{\gamma}} \bar{\boldsymbol{D}}^p + \dot{\gamma} \left\{ \Phi_{S f} \boldsymbol{N} - \frac{1}{3} \Phi_{p f} \boldsymbol{I} \right\} \quad (28)$$

$$\boldsymbol{D}_3 = \frac{\dot{\gamma} \overset{\circ}{p}}{\dot{\gamma}} \bar{\boldsymbol{D}}^p + \dot{\gamma} \left\{ \Phi_{S p} \boldsymbol{N} - \frac{1}{3} \Phi_{p p} \boldsymbol{I} \right\} \quad (29)$$

$$\boldsymbol{D}_4 = \frac{\dot{\gamma} \overset{\circ}{S}}{\dot{\gamma}} \bar{\boldsymbol{D}}^p + \dot{\gamma} \left\{ \Phi_{S S} \boldsymbol{N} - \frac{\Phi_S}{S} \boldsymbol{N} - \frac{1}{3} \Phi_{p S} \boldsymbol{I} \right\} \quad (30)$$

$$\boldsymbol{D}_5 = \frac{\dot{\gamma} \overset{\circ}{s}}{\dot{\gamma}} \bar{\boldsymbol{D}}^p + \dot{\gamma} \left\{ \Phi_{S s} \boldsymbol{N} - \frac{1}{3} \Phi_{p s} \boldsymbol{I} \right\} \quad (31)$$

$$\boldsymbol{D}_6 = \frac{\dot{\gamma} \overset{\circ}{\theta}}{\dot{\gamma}} \bar{\boldsymbol{D}}^p + \dot{\gamma} \left\{ \Phi_{S \theta} \boldsymbol{N} - \frac{1}{3} \Phi_{p \theta} \boldsymbol{I} \right\} \quad (32)$$

$$d_7 = \dot{\gamma} \frac{\Phi_S}{S} \quad (33)$$

where $\Phi_S \equiv \partial_S \Phi$ and $\Phi_p \equiv \partial_p \Phi$ and subscripts denote partial derivatives. From Equation (26), we note that $\bar{\boldsymbol{D}}^p$ can be expressed in terms of $[\overset{\circ}{p}, \overset{\circ}{S}, \overset{\circ}{\theta}]$ and $\overset{\circ}{\boldsymbol{T}}'$ if $[\overset{\circ}{\sigma}_m, \overset{\circ}{f}, \overset{\circ}{s}]$ can be expressed in terms of $[\overset{\circ}{p}, \overset{\circ}{S}, \overset{\circ}{\theta}]$. Indeed, let us design-differentiate the consistency condition (Equation (6)) to derive the following:

$$\overset{\circ}{\Phi} = \overline{\Phi(\sigma_m, f, p, S)} = 0 \quad (34)$$

where $\overset{\circ}{\Phi}$ is expressed in terms of $\overset{\circ}{\sigma}_m$, $\overset{\circ}{f}$, $\overset{\circ}{p}$, $\overset{\circ}{S}$ and $\overset{\circ}{s}$ by taking partial derivatives of $\overset{\circ}{\Phi}$ with respect to its arguments. The resulting equation takes the following form:

$$\begin{aligned} c_1 \overset{\circ}{\sigma}_{mn+1} + c_2 \overset{\circ}{f}_{n+1} + c_3 \overset{\circ}{s}_{n+1} \\ = c_5 \overset{\circ}{p}_{n+1} + c_6 \overset{\circ}{S}_{n+1} + c_7 \overset{\circ}{\theta}_{n+1} \end{aligned} \quad (35)$$

where the constants c_1, \dots, c_7 can be easily evaluated. Note that for the Gurson model $c_3 = c_7 = 0$.

The sensitivities $\overset{\circ}{f}$ and $\overset{\circ}{s}$ can be evaluated by design differentiation of Equations (12) and (11), respectively:

$$\frac{\partial \overset{\circ}{f}}{\partial t} = -\overset{\circ}{f} \operatorname{tr} \overset{\circ}{\bar{D}}^p + (1 - \overset{\circ}{f}) \operatorname{tr} \overset{\circ}{\bar{D}}^p \quad (36)$$

$$\frac{\partial \overset{\circ}{s}}{\partial t} = g_{\sigma_m} \overset{\circ}{\sigma}_m + g_s \overset{\circ}{s} + g_{\theta} \overset{\circ}{\theta} \quad (37)$$

where g is the hardening function and $\operatorname{tr} \overset{\circ}{\bar{D}}^p = -\frac{\overset{\circ}{\sigma}}{\overset{\circ}{\gamma} \partial_p \overset{\circ}{\Phi}}$. An Euler-backward time integration scheme is applied to the above evolution equations resulting in the following:

$$\begin{aligned} b_1 \overset{\circ}{\sigma}_{mn+1} + b_2 \overset{\circ}{f}_{n+1} + b_3 \overset{\circ}{s}_{n+1} \\ = b_4 + b_5 \overset{\circ}{p}_{n+1} + b_6 \overset{\circ}{S}_{n+1} + b_7 \overset{\circ}{\theta}_{n+1} \end{aligned} \quad (38)$$

$$a_1 \overset{\circ}{\sigma}_{mn+1} + a_2 \overset{\circ}{s}_{n+1} = a_3 + a_4 \overset{\circ}{\theta}_{n+1} \quad (39)$$

where the constants a_1, \dots, a_4 , b_1, \dots, b_7 can be easily computed.

Equations (35), (38) and (39) can be solved for $\overset{\circ}{\sigma}_{mn+1}$, $\overset{\circ}{f}_{n+1}$ and $\overset{\circ}{s}_{n+1}$ in terms of $\overset{\circ}{p}_{n+1}$, $\overset{\circ}{S}_{n+1}$ and $\overset{\circ}{\theta}_{n+1}$ to yield the following:

$$\begin{pmatrix} \overset{\circ}{\sigma}_{mn+1} \\ \overset{\circ}{f}_{n+1} \\ \overset{\circ}{s}_{n+1} \end{pmatrix} = \begin{bmatrix} \mathcal{M}_{11} & \mathcal{M}_{12} & \mathcal{M}_{13} \\ \mathcal{M}_{21} & \mathcal{M}_{22} & \mathcal{M}_{23} \\ \mathcal{M}_{31} & \mathcal{M}_{32} & \mathcal{M}_{33} \end{bmatrix} \begin{pmatrix} \overset{\circ}{p}_{n+1} \\ \overset{\circ}{S}_{n+1} \\ \overset{\circ}{\theta}_{n+1} \end{pmatrix} + \begin{pmatrix} m_1 \\ m_2 \\ m_3 \end{pmatrix} \quad (40)$$

where the 3×3 matrix \mathcal{M} and the scalars m_1 , m_2 , m_3 are constants. Using the above solution for $\overset{\circ}{\sigma}_{mn+1}$, $\overset{\circ}{f}_{n+1}$ and

$\overset{\circ}{s}_{n+1}$ in terms of $\overset{\circ}{p}_{n+1}$, $\overset{\circ}{S}_{n+1}$ and $\overset{\circ}{\theta}_{n+1}$ along with Equation (26), one can relate $\overset{\circ}{\bar{D}}^p_{n+1}$ to $\overset{\circ}{p}_{n+1}$, $\overset{\circ}{S}_{n+1}$, $\overset{\circ}{\theta}_{n+1}$ and $\overset{\circ}{\bar{T}}'_{n+1}$. Let this relation be expressed as follows:

$$\begin{aligned} \overset{\circ}{\bar{D}}^p_{n+1} = & \mathbf{D}'_1 \overset{\circ}{p}_{n+1} + \mathbf{D}'_2 \overset{\circ}{S}_{n+1} + \mathbf{D}'_3 \overset{\circ}{\theta}_{n+1} \\ & + \mathbf{D}'_4 + d_7 \overset{\circ}{\bar{T}}'_{n+1} \end{aligned} \quad (41)$$

where \mathbf{D}'_1 , \mathbf{D}'_2 , \mathbf{D}'_3 , \mathbf{D}'_4 are known second order tensors and d_7 , a scalar, defined earlier.

The dependence of $\overset{\circ}{\bar{T}}'_{n+1}$ on $\overset{\circ}{F}^e_{n+1}$ is derived by design-differentiation of the hyperelastic model of Equation (2) as follows:

$$\overset{\circ}{\bar{T}}'_{n+1} = \mathcal{L}^e [\overset{\circ}{\bar{E}}^e_{n+1}] + \overset{\circ}{\mathcal{L}}^e [\overset{\circ}{\bar{E}}^e_{n+1}] \quad (42)$$

$$\overset{\circ}{\mathcal{L}}^e = 2 \overset{\circ}{\mu} \mathcal{I} + \left(\overset{\circ}{\kappa} - \frac{2}{3} \overset{\circ}{\mu} \right) \mathcal{I} \otimes \mathcal{I} \quad (43)$$

where from Badrinarayanan and Zabaras (1996) it is known that:

$$\overset{\circ}{\bar{E}}^e_{n+1} = 4(\mathbf{U}^e_{n+1} + \mathbf{I})^{-1} \overset{\circ}{\mathbf{U}}^e_{n+1} (\mathbf{U}^e_{n+1} + \mathbf{I})^{-1} \quad (44)$$

$$\overset{\circ}{\mathbf{U}}^e_{n+1} = \operatorname{sym} \left\{ (\mathbf{U}^e_{n+1})^{-1} \operatorname{sym} \left((\mathbf{F}^e_{n+1})^T \overset{\circ}{\mathbf{F}}^e_{n+1} \right) \right\} \quad (45)$$

The second term on the RHS of Equation (42) results in a linear relation of $\overset{\circ}{\bar{T}}'_{n+1}$ with $\overset{\circ}{f}_{n+1}$ and $\overset{\circ}{\theta}_{n+1}$. Using the second equation in the linear system in Equation (40), one can substitute $\overset{\circ}{f}_{n+1}$ in terms of $\overset{\circ}{p}_{n+1}$, $\overset{\circ}{S}_{n+1}$ and $\overset{\circ}{\theta}_{n+1}$. We can then, in general, using Equations (42)-(45), write the following relation between $\overset{\circ}{\bar{T}}'_{n+1}$ and the set $\{\overset{\circ}{F}^e_{n+1}, \overset{\circ}{p}_{n+1}, \overset{\circ}{S}_{n+1}, \overset{\circ}{\theta}_{n+1}\}$:

$$\begin{aligned} \overset{\circ}{\bar{T}}'_{n+1} = & \mathbf{E}_1 \overset{\circ}{p}_{n+1} + \mathbf{E}_2 \overset{\circ}{S}_{n+1} + \mathbf{E}_3 \overset{\circ}{\theta}_{n+1} \\ & + \mathbf{E}_4 + \mathcal{E}_5 [\overset{\circ}{F}^e_{n+1}] \end{aligned} \quad (46)$$

where $\mathbf{E}_1, \mathbf{E}_2, \mathbf{E}_3, \mathbf{E}_4$ are known second order tensors and \mathcal{E}_5 a known fourth order tensor. Using Equation (46), Equation (41) can be simplified as follows:

$$\overset{\circ}{\bar{\mathbf{D}}}_{n+1}^p = \mathbf{D}_1'' \overset{\circ}{\bar{p}}_{n+1} + \mathbf{D}_2'' \overset{\circ}{\bar{\mathcal{S}}}_{n+1} + \mathbf{D}_3'' \overset{\circ}{\bar{\theta}}_{n+1} + \mathbf{D}_4'' + \mathcal{D}_5''[\overset{\circ}{\mathbf{F}}_{n+1}^e] \quad (47)$$

where $\mathbf{D}_1'', \mathbf{D}_2'', \mathbf{D}_3'', \mathbf{D}_4''$ are known second order tensors and $\mathcal{D}_5'' = d_7 \mathcal{E}_5$.

The sensitivities $\overset{\circ}{\bar{\mathcal{S}}}$ and $\overset{\circ}{\bar{p}}$, are evaluated as follows:

$$\overset{\circ}{\bar{\mathcal{S}}} = \frac{\overset{\circ}{\bar{\mathbf{T}}}}{(\sqrt{\overset{\circ}{\bar{\mathbf{T}}} \cdot \overset{\circ}{\bar{\mathbf{T}}}})} = \frac{1}{\bar{\mathcal{S}}} (\overset{\circ}{\bar{\mathbf{T}}} \cdot \overset{\circ}{\bar{\mathbf{T}}}) \quad (48)$$

$$\overset{\circ}{\bar{p}} = -\text{tr} \overset{\circ}{\bar{\mathbf{T}}}/3 \quad (49)$$

where $\overset{\circ}{\bar{\mathbf{T}}}'$ is the deviatoric part of the sensitivity of the rotation neutralized Cauchy stress. Substitution of Equation (46) in the two equations above results in two linear equations that can be solved to compute $\overset{\circ}{\bar{p}}$ and $\overset{\circ}{\bar{\mathcal{S}}}$ in terms of $\overset{\circ}{\mathbf{F}}^e$ and $\overset{\circ}{\theta}$. The derived functional form of $\overset{\circ}{\bar{\mathcal{S}}}_{n+1}$ as well as $\overset{\circ}{\bar{p}}_{n+1}$ can finally be expressed as follows:

$$\overset{\circ}{\bar{\mathcal{S}}}_{n+1} = a_{n+1} + b_{n+1} \overset{\circ}{\theta}_{n+1} + k_{n+1}^1(\overset{\circ}{\mathbf{F}}_{n+1}^e) \quad (50)$$

$$\overset{\circ}{\bar{p}}_{n+1} = c_{n+1} + d_{n+1} \overset{\circ}{\theta}_{n+1} + k_{n+1}^2(\overset{\circ}{\mathbf{F}}_{n+1}^e) \quad (51)$$

where $a_{n+1}, b_{n+1}, c_{n+1}, d_{n+1}$ are known constants and k_{n+1}^1 and k_{n+1}^2 are known scalar-valued function of a second order tensor, all defined at time t_{n+1} . Substitution of these relations in Equation (47) results in the following final expression:

$$\overset{\circ}{\bar{\mathbf{D}}}_{n+1}^p = \mathcal{A}_{n+1}[\overset{\circ}{\mathbf{F}}_{n+1}^e] + \mathbf{A}_{n+1} \overset{\circ}{\theta}_{n+1} + \mathbf{B}_{n+1} \quad (52)$$

$\mathbf{A}_{n+1}, \mathbf{B}_{n+1}$ are known second order tensors and \mathcal{A}_{n+1} is a known fourth order tensor defined at t_{n+1} .

An Euler-backward time integration scheme over (t_n, t_{n+1}) applied to the evolution equations for the sensitivities of the plastic deformation gradient (Equation (24))

yields:

$$\overset{\circ}{\mathbf{F}}_{n+1}^p (\overset{\circ}{\mathbf{F}}_{n+1}^p)^{-1} = \Delta \mathbf{F}^p \overset{\circ}{\mathbf{F}}_n^p (\overset{\circ}{\mathbf{F}}_n^p)^{-1} (\Delta \mathbf{F}^p)^{-1} + \Delta t \overset{\circ}{\bar{\mathbf{D}}}_{n+1}^p \quad (53)$$

where from the constitutive sub-problem of the direct problem (Weber and Anand (1990)),

$$\Delta \mathbf{F}^p = \mathbf{F}_{n+1}^p (\overset{\circ}{\mathbf{F}}_n^p)^{-1} = \exp(\Delta t \overset{\circ}{\bar{\mathbf{D}}}_{n+1}^p) \quad (54)$$

with $\Delta t = t_{n+1} - t_n$.

Substituting Equation (52) in Equation (53), one obtains the desired linear relationship between $\overset{\circ}{\mathbf{F}}_{n+1}^p$ and $[\overset{\circ}{\mathbf{F}}_{n+1}^e, \overset{\circ}{\theta}_{n+1}]$.

Linear relation between $\overset{\circ}{\mathbf{F}}_{n+1}^e$ and $[\overset{\circ}{\mathbf{F}}_{n+1}, \overset{\circ}{\theta}_{n+1}]$: Starting from the multiplicative decomposition of the deformation gradient, one can write

$$\overset{\circ}{\mathbf{F}}_{n+1} = \overset{\circ}{\mathbf{F}}_{n+1}^e \overset{\circ}{\mathbf{F}}_{n+1}^p \overset{\circ}{\mathbf{F}}_{n+1}^\theta + \overset{\circ}{\mathbf{F}}_{n+1}^e \overset{\circ}{\mathbf{F}}_{n+1}^p \overset{\circ}{\mathbf{F}}_{n+1}^\theta \quad (55)$$

The evolution equation for $\overset{\circ}{\mathbf{F}}_{n+1}^\theta$ is derived in Ganapathysubramanian and Zabararas (2002) as follows:

$$\overset{\circ}{\mathbf{F}}_{n+1}^\theta (\overset{\circ}{\mathbf{F}}_{n+1}^\theta)^{-1} = \beta \overset{\circ}{\theta}_{n+1} \mathbf{I} \quad (56)$$

Equation (55) can then be simplified as,

$$(\overset{\circ}{\mathbf{F}}_{n+1}^e)^{-1} \left(\overset{\circ}{\mathbf{F}}_{n+1} \overset{\circ}{\mathbf{F}}_{n+1}^{-1} \right) \overset{\circ}{\mathbf{F}}_{n+1}^e = (\overset{\circ}{\mathbf{F}}_{n+1}^e)^{-1} \overset{\circ}{\mathbf{F}}_{n+1}^e + \overset{\circ}{\mathbf{F}}_{n+1}^p (\overset{\circ}{\mathbf{F}}_{n+1}^p)^{-1} + \beta \overset{\circ}{\theta}_{n+1} \mathbf{I} \quad (57)$$

assuming β is a constant.

Substitution of the earlier obtained linear relationship between $\overset{\circ}{\mathbf{F}}_{n+1}^p$ and $[\overset{\circ}{\mathbf{F}}_{n+1}^e, \overset{\circ}{\theta}_{n+1}]$ in Equation (57) results in the desired linear relationship that can be expressed as:

$$\overset{\circ}{\mathbf{F}}_{n+1}^e = \mathcal{B}(\mathbf{V}_{n+1}) \left[\overset{\circ}{\mathbf{F}}_{n+1}^e \right] + \mathbf{A} \left(\mathbf{V}_{n+1}, \overset{\circ}{\mathbf{V}}_n \right) + \mathbf{B}(\mathbf{V}_{n+1}) \overset{\circ}{\theta}_{n+1} \quad (58)$$

where \mathbf{A} and \mathbf{B} are known second order tensor functions and \mathbf{B} , a known fourth order tensor function. The arguments in these functions are here given in terms of the set $\mathbf{V} \equiv [\mathbf{T}, s, f, \mathbf{F}^p]$ (at time t_{n+1}) and its sensitivity $\overset{\circ}{\mathbf{V}}$ (at time t_n).

Linear relation between $\overset{\circ}{\mathbf{T}}_{n+1}$ and $[\overset{\circ}{\mathbf{F}}_{n+1}, \overset{\circ}{\theta}_{n+1}]$: The relationship between $\overset{\circ}{\mathbf{T}}$ and $[\overset{\circ}{\mathbf{F}}_{n+1}, \overset{\circ}{\theta}_{n+1}]$ is developed in Srikanth and Zabarar (2000). It is given as follows:

$$\begin{aligned} \overset{\circ}{\mathbf{T}} &= (\det(\mathbf{U}^e))^{-1} \mathbf{R}^e \overset{\circ}{\mathbf{T}} \mathbf{R}^{eT} - \text{tr} \overset{\circ}{\mathbf{E}}^e \mathbf{T} \\ &+ \left\{ \overset{\circ}{\mathbf{R}}^e \mathbf{R}^{eT} \mathbf{T} - \mathbf{T} \overset{\circ}{\mathbf{R}}^e \mathbf{R}^{eT} \right\} \end{aligned} \quad (59)$$

where

$$\begin{aligned} \overset{\circ}{\mathbf{R}}^e \mathbf{R}^{eT} &= \overset{\circ}{\mathbf{F}}^e \mathbf{F}^{e-1} \\ &- \mathbf{R}^{e \text{sym}} \left(\left\{ \mathbf{U}^{e-1 \text{sym}} \left(\mathbf{F}^{e-1} \overset{\circ}{\mathbf{F}}^e \right) \right\} \right) \mathbf{U}^{e-1} \mathbf{R}^{eT} \end{aligned} \quad (60)$$

Substitution of the linear relation between $\overset{\circ}{\mathbf{F}}_{n+1}^e$ and $[\overset{\circ}{\mathbf{F}}_{n+1}, \overset{\circ}{\theta}_{n+1}]$ (Equation (58)) in Equation (59), results in a linear relation between $\overset{\circ}{\mathbf{T}}_{n+1}$ and $[\overset{\circ}{\mathbf{F}}_{n+1}, \overset{\circ}{\theta}_{n+1}]$.

Postprocessing operations: Calculation of $\overset{\circ}{\mathbf{F}}_{n+1}^e$ and $\overset{\circ}{p}_{n+1}$, $\overset{\circ}{S}_{n+1}$, $\overset{\circ}{\sigma}_{mn+1}$, $\overset{\circ}{f}_{n+1}$, $\overset{\circ}{s}_{n+1}$ given $[\overset{\circ}{\mathbf{F}}_{n+1}, \overset{\circ}{\theta}_{n+1}]$: Many of the above presented linear relations can be used for postprocessing operations once the calculation of $\overset{\circ}{\mathbf{F}}_{n+1}$ and $\overset{\circ}{\theta}_{n+1}$ is complete within a time step.

With $\overset{\circ}{\mathbf{F}}_{n+1}^e$ computed from Equation (58), one can evaluate $\overset{\circ}{S}_{n+1}$ and $\overset{\circ}{p}_{n+1}$ from Equations (50) and (51), respectively. Finally, Equation (40) can be used to compute $\overset{\circ}{\sigma}_{mn+1}$, $\overset{\circ}{f}_{n+1}$ and $\overset{\circ}{s}_{n+1}$.

Calculation of the linear relation between $\overset{\circ}{\mathcal{W}}_{mech,n+1}$ and $[\overset{\circ}{\mathbf{F}}_{n+1}, \overset{\circ}{\theta}_{n+1}]$: Using Equation (13), we can compute $\overset{\circ}{\mathcal{W}}_{mech}$ as follows:

$$\overset{\circ}{\mathcal{W}}_{mech} = \omega [(1-f)(\overset{\circ}{\sigma}_m \overset{\circ}{\epsilon}^p + \sigma_m \overset{\circ}{\epsilon}^p) - f \sigma_m \overset{\circ}{\epsilon}^p] \quad (61)$$

The sensitivity field $\overset{\circ}{\epsilon}^p$ can be easily computed by design differentiation of Equation (10) in terms of the sensitivity fields $\overset{\circ}{\sigma}_{mn+1}$, $\overset{\circ}{s}_{n+1}$ and $\overset{\circ}{\theta}_{n+1}$. With a known linear relation between $\overset{\circ}{\mathbf{F}}_{n+1}^e$ and $[\overset{\circ}{\mathbf{F}}_{n+1}, \overset{\circ}{\theta}_{n+1}]$ (Equation (58)), Equations (50) and (51) can provide the linear relations of $\overset{\circ}{S}_{n+1}$ and $\overset{\circ}{p}_{n+1}$ with $[\overset{\circ}{\mathbf{F}}_{n+1}, \overset{\circ}{\theta}_{n+1}]$. Introducing these linear relations in Equation (40) will lead to the linear relations between $\overset{\circ}{\sigma}_{mn+1}$, $\overset{\circ}{s}_{n+1}$ and $[\overset{\circ}{\mathbf{F}}_{n+1}, \overset{\circ}{\theta}_{n+1}]$ and thus the required linear relation between $\overset{\circ}{\epsilon}^p$ and $[\overset{\circ}{\mathbf{F}}_{n+1}, \overset{\circ}{\theta}_{n+1}]$.

Thermal sensitivity problem

The thermal sensitivity problem is solved in a similar fashion to the one described in Ganapathysubramanian and Zabarar (2002). We note, however, that here ρc and K are functions of the void fraction, f , and temperature, θ . The sensitivity thermal evolution equation is obtained by the design differentiation of the energy equation in the work-piece. A weak form of the thermal sensitivity equation is then posed on the deformed configuration \mathcal{B}_{n+1} . Let ϑ represent an admissible sensitivity temperature field expressed over \mathcal{B}_{n+1} . The variational form of the sensitivity energy problem is posed as:

$$\begin{aligned} &\int_{\mathcal{B}_{n+1}} \left(\frac{\rho c}{\Delta t} (\overset{\circ}{\theta}_{n+1} - \overset{\circ}{\theta}_n) + \frac{(\rho c)_\theta}{\Delta t} (\theta_{n+1} - \theta_n) \overset{\circ}{\theta}_{n+1} \right) \vartheta dV \\ &+ \int_{\mathcal{B}_{n+1}} \left(K \nabla_{n+1} \overset{\circ}{\theta}_{n+1} + K_\theta \overset{\circ}{\theta}_{n+1} \nabla_{n+1} \theta_{n+1} \right) \cdot \nabla_{n+1} \vartheta dV + \\ &\int_{\partial \mathcal{B}_{n+1}} [\overset{\circ}{\mathbf{q}}_{n+1}] \cdot \mathbf{n} dA \\ &= \int_{\mathcal{B}_{n+1}} \left(\overset{\circ}{\mathcal{W}}_{mech,n+1} \nabla_{n+1} \mathbf{q}_{n+1} \cdot \mathbf{L}_{n+1} \right) \vartheta dV \\ &- \int_{\mathcal{B}_{n+1}} \left(\mathbf{L}_{n+1}^T \mathbf{q}_{n+1} + K_f \overset{\circ}{f}_{n+1} \nabla_{n+1} \theta_{n+1} \right) \cdot \nabla_{n+1} \vartheta dV \\ &- \int_{\mathcal{B}_{n+1}} \frac{(\rho c)_f}{\Delta t} (\theta_{n+1} - \theta_n) \overset{\circ}{f}_{n+1} \vartheta dV \end{aligned}$$

Appropriate thermal sensitivity boundary conditions need to be applied for the solution of the above weak problem.

Evaluation of gradients from the computed sensitivities

One can compute the gradients $\frac{\partial \Omega}{\partial \beta_i}$ using the continuum based sensitivity fields as follows:

$$\frac{\partial \Omega}{\partial \beta_i} = \frac{\overset{\circ}{\Omega}(\mathbf{x}, t, \beta_1, \beta_2, \dots, \beta_n, 0, \dots, 0, \Delta \beta_i, 0, \dots, 0)}{\Delta \beta_i} \quad (62)$$

Thus to compute $\nabla \Omega$, we need to solve a total of $n + 1$ problems, one nonlinear direct problem and n linear sensitivity problems. We have performed an extensive comparison of sensitivity fields computed with the above presented CSM with the results obtained by the FDM. These studies will be reported in a forthcoming publication.

NUMERICAL EXAMPLES

In this section, we present preliminary numerical examples that utilize sensitivity fields computed with the CSM in gradient-based optimization implementation of the computational design of industrial forming processes. The first example deals with the design of preforms for closed die forging processes. The second example deals with the minimization of porosity near the central axis of an extrusion process.

In all the examples presented here, when process constraints are introduced, a penalty method is used to convert the constrained optimization problem to an unconstrained one. A quasi-Newton type method is used to solve the unconstrained minimization problem with the BFGS scheme.

Convective boundary conditions are imposed on all free surfaces, i.e. surfaces other than symmetry axes, that are not in contact. The convective heat transfer coefficient is taken as $h = 6.7 \text{ W}/(\text{m}^2 - \text{K})$. The ambient (atmospheric) temperature is taken as 298 K. For simplicity, the die is assumed to be rigid and isothermal (at room temperature) and no heat transfer is considered between the die and the workpiece. The computational process parameters for both examples are the same and are tabulated in Table 1.

Preform design for closed-die forging

Constant elastic properties: Example 1a The objective here is to design the volume and the free surface of a cylindrical preform of height 2.0 mm, that when compressed with a closed forging die, fills the die completely with minimum or no flash, after a specified stroke of 0.65 mm. The friction coefficient between the die and workpiece is taken as 0.1. The desired final radius around the flash is taken as 1.2 mm and the desired height at $r = 0$ as 0.7 mm.

Table 1. SIMULATION PARAMETERS

Parameter	Value
Energy error norm	1.00×10^{-4}
Displacement L_2 error norm	1.00×10^{-4}
Normal penalty in direct contact problem	$1.00 \times 10^{+5}$
Tangent penalty in direct contact problem	$1.00 \times 10^{+4}$
Normal penalty in sensitivity contact problem	$1.00 \times 10^{+8}$
Tangent penalty in sensitivity contact problem	$1.00 \times 10^{+7}$
Tolerance for gap	1.00×10^{-5}
Tolerance for slip	1.00×10^{-4}
Tolerance for friction	1.00×10^{-4}

The workpiece material is taken to be Fe-2 % Si at an initial temperature of 1273 K. The material has a constitutive behavior defined in Anand (1985). The constitutive model used (flow function and hardening law, respectively) is defined as follows:

$$f(\sigma_m, s, \theta) = A \exp\left(-\frac{Q}{R\theta}\right) \left[\sinh\left(\xi \frac{\sigma_m}{s}\right)\right]^{1/m} \quad (63)$$

$$h(\sigma, s, \theta) = h_0 \left|1 - \frac{s}{s^*}\right|^a \quad (64)$$

where

$$s^* = \tilde{s} \left[\frac{f(\sigma_m, s, \theta)}{A} \exp\left(\frac{Q}{R\theta}\right) \right]^n \quad (65)$$

The values of the mechanical and thermal parameters are given in Table 2.

The particular die for this problem is defined as follows:

$$\left\{ \begin{array}{l} r(\eta) = 1.6 * (1 - \eta) \\ \left\{ \begin{array}{ll} 0.9 & \eta \in [0, 0.25] \\ 4.1 - 25.6 * \eta + 51.2 * \eta^2 & \eta \in [0.25, 0.3125] \\ 10.35 - 105.6 * \eta + \\ 371.2 * \eta^2 - 409.6 * \eta^3 & \eta \in [0.3125, 0.375] \\ 1.35 & \eta \in [0.375, 0.4375] \end{array} \right. \\ z(\eta) = \left\{ \begin{array}{ll} -128.5 + 828.8 * \eta - \\ 1753.6 * \eta^2 + 1228.8 * \eta^3 & \eta \in [0.4375, 0.5] \\ 9.1 - 28.8 * \eta + 25.6 * \eta^2 & \eta \in [0.5, 0.5625] \\ 1.0 & \eta \in [0.5625, 1] \end{array} \right. \end{array} \right.$$

The free surface $R_{\beta}(\alpha)$ of the preform is represented with a degree 6 Bézier curve (with 7 Bernstein basis functions). Using the restriction $R'_{\beta}(0) = 0$, the representation

Table 2. MATERIAL PARAMETERS FOR Fe-2 % Si AT A TEMPERATURE OF 1273 K.

Material Parameter	Value
A	$6.346 \times 10^{11} \text{ sec}^{-1}$
Q/R	$3.756916 \times 10^4 \text{ K}^{-1}$
ξ	3.25
m	0.1956
s_0	66.1 MPa
h_0	3093.1 MPa
a	1.5
\tilde{s}	125.1 MPa
n	0.06869
μ	37.23 GPa
κ	194.45 GPa
β	$11.80 \times 10^{-6} / \text{K}$
K	80.0 N/(secs-K)
ρc	$2.47 \times 10^6 \text{ J}/(\text{m}^3\text{-K})$
ω	0.90

of R_{β} can be defined with 6 independent design variables β_i , $i = [1 \dots 6]$ as follows:

$$R_{\beta}(\alpha) = \sum_{i=1}^6 \beta_i \phi_i(\alpha)$$

$$Z = 1.5\alpha \quad 0 \leq \alpha \leq 1 \quad (66)$$

where Z represents the axial coordinate, α represents the normalized radial coordinate and the basis functions are given as

$$\begin{aligned} \phi_1 &= (1.0 - \alpha)^5 (1.0 + 5.0\alpha), & \phi_2 &= 15.0 (1.0 - \alpha)^4 \alpha^2 \\ \phi_3 &= 20.0 (1.0 - \alpha)^3 \alpha^3, & \phi_4 &= 15.0 (1.0 - \alpha)^2 \alpha^4 \\ \phi_5 &= 6.0 (1.0 - \alpha) \alpha^5, & \phi_6 &= \alpha^6 \end{aligned} \quad (67)$$

The finite dimensional optimization problem is posed as follows:

$$\min_{\beta} \mathcal{F}(\beta) = \frac{1}{N} \sum_{i=1}^N \sum_{j=1}^2 (x_j^i(\beta) - x_j^{desired})^2 \quad (68)$$

where $\beta = \{\beta_1, \dots, \beta_6\}$, $(x_1^{desired}, x_2^{desired})$ defines the desired boundary and N refers to the number of nodes on the

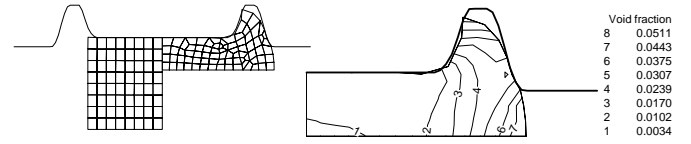


Figure 2. INITIAL GUESS PREFORM SHAPE, THE FINAL PRODUCT USING THIS GUESS AND THE DISTRIBUTION OF VOID FUNCTION IN THE FINAL PRODUCT FOR A CLOSED DIE FORGING PROCESS (EXAMPLE 1a).

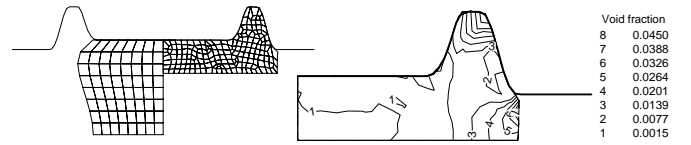


Figure 3. OPTIMAL PREFORM SHAPE, THE FINAL PRODUCT USING THIS PREFORM AND THE DISTRIBUTION OF THE VOID FRACTION FOR A CLOSED DIE FORGING PROCESS (EXAMPLE 1a).

free surface and regions in contact of the final product.

Figure 2 shows the quarter geometry of the initial guess preform (a right circular cylinder of radius 0.8 mm and height of 2 mm). Its discretization is performed with a mesh of 8×8 (quarter geometry) that is kept similar for all subsequent preforms. Also shown is the final product shape obtained using this guessed preform. Figure 3 shows the optimal preform and the final product shape achieved using this optimal preform. The variation of the objective function with the iteration index is shown in Figure 4. It can also be observed in Figure 2 that the void fraction in localized areas is more than the initial void fraction of 5%. The volume of the optimum preform was evaluated as 2.6027 mm^3 , whereas the volume enclosed by the die cavity is 2.5353 mm^3 .

Varying elastic properties: Example 1b A design problem similar to the previous one, but with a different material model to account for variable elastic moduli is carried out. The process parameters are the same as the ones used in the previous example.

The process was studied for a workpiece made of 2024-T351 Aluminum alloy with an initial void fraction of $f_0 = 5\%$ and an initial temperature of 300 K. The flow and

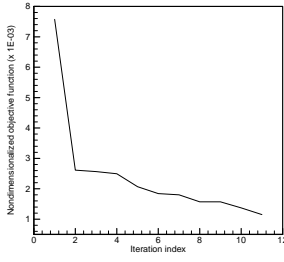


Figure 4. VARIATION OF THE NONDIMENSIONALIZED OBJECTIVE FUNCTION WITH ITERATION INDEX FOR A CLOSED DIE FORGING PROCESS (EXAMPLE 1a).

hardening functions proposed by Lindholm and Johnson are obtained from Zavalianos and Anand (1992) and take the following form. The flow function f is given as

$$f(\sigma_m, s, \theta) = \dot{\epsilon}_o \exp \left[\frac{1}{C} \left(\frac{\sigma_m}{s \left(\frac{\theta_m - \theta}{\theta_m - \theta_o} \right)^a} - 1 \right) \right] \quad (69)$$

and the state variable s is given explicitly as

$$s(t) = A + B (\epsilon_m^p)^n \quad (70)$$

where the equivalent plastic strain ϵ_m^p is defined as

$$\epsilon_m^p = \int_0^t f(\sigma_m, s, \theta) dt \quad (71)$$

The specific values of the mechanical and thermal parameters are given in Table 3.

The elastic properties are taken as follows:

$$\mu_m = \mu_{m,o} \left(1 - \xi_1 \frac{\theta - \theta_o}{\theta_m} \right) \quad (72)$$

$$\kappa_m = \kappa_{m,o} \left(1 - \xi_2 \frac{\theta - \theta_o}{\theta_m} \right) \quad (73)$$

Here, the subscript m refers to the properties of the matrix material and the subscript o refers to properties specified at the reference temperature θ_o . The method described by Budiansky (1970) was used to calculate the elastic properties $\mu = \mu(\theta, f)$ and $\kappa = \kappa(\theta, f)$ of the porous material (composite) in terms of the elastic properties of the matrix material.

Table 3. MATERIAL PARAMETERS FOR 2024-T351 Al AT AN INITIAL TEMPERATURE OF 300 K.

Material Parameter	Value
A	263.28 MPa
B	421.72 MPa
C	0.015
$\dot{\epsilon}_o$	0.577 sec ⁻¹
θ_o	300 K
θ_m	775 K
ξ_1	0.5
ξ_2	0.333
a	2
n	0.34
$\mu_{m,o}$	26 GPa
$\kappa_{m,o}$	68 GPa
β_m	22.6 × 10 ⁻⁶ / K
K	160.0 N/(secs-K)
ρ	2770 Kg/m ³
c	875 J/(Kg-K)
ω	0.90

Figure 5 shows the quarter geometry of the initial guess preform (a right circular cylinder of radius 0.8 mm and height of 2 mm) and final product shape obtained using this guessed preform. Figure 6 shows the optimal preform and the final product shape achieved using this optimal preform. The variation of the objective function with the iteration index is shown in Figure 7. The volume of the optimum preform was evaluated as 2.5446 mm³. Also shown in Figures 5 and 6 is the variation of the shear modulus in the forged product.

Die design for extrusion - Isothermal, frictionless process with ductile damage (Example 2)

Chevron defects, also known as central bursts, are gaps in the material flow that form a special category of ductile fracture. The objective here is to design the extrusion die shape so as to minimize the void fraction at the center of the extruded product. Here, we design an extrusion process with a die of area reduction of 10.7%. The initial radius of the workpiece is 0.508 mm and the initial height is 2.1 mm. The material is assumed to have an initial porosity of $f_o = 1\%$. It was extruded with a nominal displacement

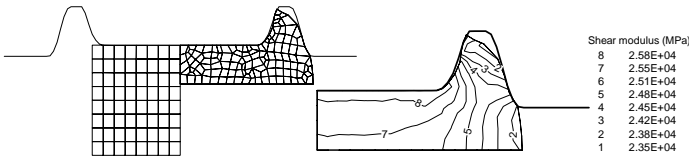


Figure 5. INITIAL GUESS PREFORM SHAPE, THE FINAL PRODUCT USING THIS GUESS AND THE DISTRIBUTION OF SHEAR MODULUS IN THE FINAL PRODUCT FOR A CLOSED DIE FORGING PROCESS (EXAMPLE 1b).

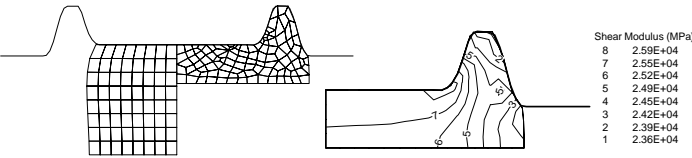


Figure 6. OPTIMAL PREFORM SHAPE, THE FINAL PRODUCT USING THIS PREFORM AND THE DISTRIBUTION OF THE SHEAR MODULUS FOR A CLOSED DIE FORGING PROCESS (EXAMPLE 1b).

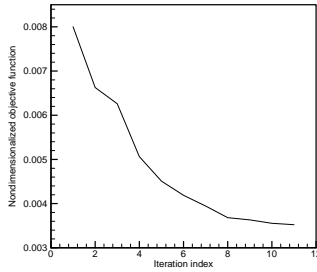


Figure 7. VARIATION OF THE NONDIMENSIONALIZED OBJECTIVE FUNCTION WITH ITERATION INDEX FOR A CLOSED DIE FORMING PROCESS (EXAMPLE 1b).

rate of 0.01 s^{-1} . A total of 120 time steps were performed to reach steady-state conditions at the exit. Frictionless conditions were assumed at the die-workpiece interface. The symmetry of the problem allowed modeling only half of the geometry. The die surface is represented by a degree nine

($n = 9$) Bézier curve as follows:

$$r(\alpha) = \sum_{i=1}^{n+1} C_i \phi_i(\alpha)$$

$$z = 0.2685(\alpha) \text{ in mm} \quad 0 \leq \alpha \leq 1 \quad (74)$$

where $C_i, i = [1 \dots (n + 1)]$, are the algebraic control parameters. The Bernstein functions $\phi_i(\alpha)$ are given as

$$\begin{aligned} \phi_1 &= (1.0 - \alpha)^9, & \phi_2 &= 9.0 (1.0 - \alpha)^8 \alpha \\ \phi_3 &= 36.0 (1.0 - \alpha)^7 \alpha^2, & \phi_4 &= 84.0 (1.0 - \alpha)^6 \alpha^3 \\ \phi_5 &= 126.0 (1.0 - \alpha)^5 \alpha^4, & \phi_6 &= 126.0 (1.0 - \alpha)^4 \alpha^5 \\ \phi_7 &= 84.0 (1.0 - \alpha)^3 \alpha^6, & \phi_8 &= 36.0 (1.0 - \alpha)^2 \alpha^7 \\ \phi_9 &= 9.0 (1.0 - \alpha) \alpha^8, & \phi_{10} &= \alpha^9 \end{aligned} \quad (75)$$

We apply the constraints (in order to obtain the same reduction for different die design parameters) that the radius and slope (with respect to the z -axis) at the inlet and exit are fixed (slope is taken as 0): $C_1 = 0.508 \text{ mm}$, $C_{10} = 0.48 \text{ mm}$, $C_2 = C_1$, and $C_9 = C_{10}$. With this selection of parameters, there are 6 die design parameters left. The initial (reference) values are arbitrary and are selected as $C_3 = 0.508$; $C_4 = 0.49$; $C_5 = 0.49$; $C_6 = 0.485$; $C_7 = 0.485$; $C_8 = 0.485$ (all of them in mm).

The functional form for the strain rate is a power law model with material rate sensitivity m , and the matrix material is assumed not to harden

$$f(\sigma_m, s) = \dot{\epsilon}_0 \left\{ \frac{\sigma_m}{s} \right\}^{1/m} \quad (76)$$

where $\dot{\epsilon}_0 = 10^{-03} \text{ sec}^{-1}$, $m = 0.05$ and $s = 150 \text{ MPa}$.

The finite dimensional optimization problem is posed as follows:

$$\min_{\beta} \mathcal{F}(\beta) = \frac{1}{N} \sum_{i=1}^N (f^i(\beta))^2 \quad (77)$$

where $\beta = \{\beta_1, \dots, \beta_6\}$, f^i is the void fraction. The area of interest is defined as a cylinder of radius 0.2 mm about the z - axis. N refers to the total number of sampling nodal points in the region of interest. A perturbation of 10^{-3} mm is used for evaluating the sensitivities with respect to the die shape.

Figure 8 shows the geometry of the initial workpiece (a right

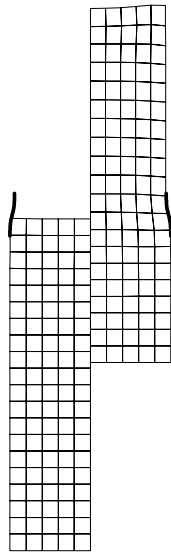


Figure 8. INITIAL GUESS DIE SHAPE AND THE FINAL EXTRUDED PRODUCT USING THIS GUESS FOR AN ISOTHERMAL, FRICTIONLESS EXTRUSION PROCESS (EXAMPLE 2).

circular cylinder of radius 0.508 mm and height of 2.1 mm) along with its discretization. Observe, in Figure 9, that the extruded product using the guess die shape has a void fraction $\geq 1\%$, the initial void fraction (e.g. look for the contour number 6). Figure 9 also shows the distributions of the void fraction in the extruded product (obtained using the optimal die shape). The void fraction in the region of interest has dramatically decreased (compared to the distribution using the guess die shape). In fact, the void fraction in this region (and elsewhere) is $< 1\%$. Also note that the void fraction in the periphery of the workpiece has increased compared to that of the initial product, even though it is much lower than the initial void fraction. The variation of the nondimensionalized objective function with the iteration index is shown in Figure 10. Shown in the same figure is the variation of the die shape for different optimization iterations.

CONCLUSIONS

This work can be viewed as a step towards realistic process modelling and design of a general class of metal forming processes. The CSM-based computed sensitivities were utilized in a gradient-based constraint optimization framework to design dies and preforms in a variety of deformation processes including forging and extrusion. The ob-

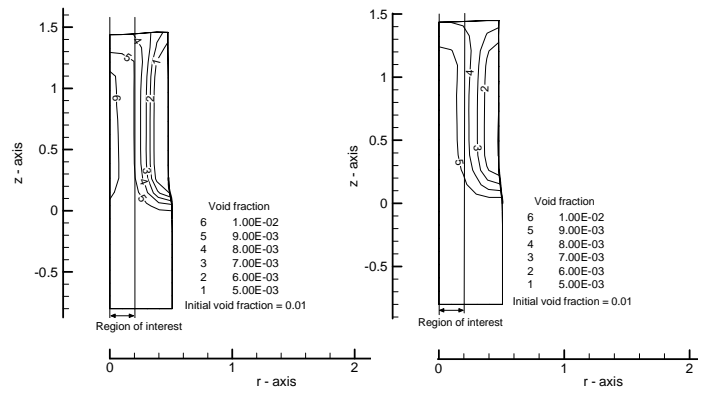


Figure 9. INITIAL AND OPTIMAL DISTRIBUTION OF VOID FRACTION IN THE FINAL PRODUCT FOR AN EXTRUSION PROCESS (EXAMPLE 2).

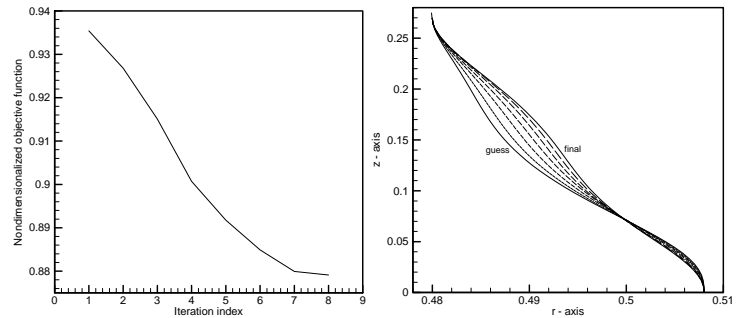


Figure 10. VARIATION OF THE NONDIMENSIONALIZED OBJECTIVE FUNCTION WITH ITERATION INDEX AND DIE SHAPES FOR DIFFERENT OPTIMIZATION ITERATIONS (EXAMPLE 2).

tained results demonstrated the significant differences from the corresponding design of processes for dense materials as well as the importance of accounting in the design process for deformation induced volumetric changes as well as for the variation of elastic properties with the evolving material state.

ACKNOWLEDGMENT

The work presented here was funded by AFOSR (grant F49620-00-1-0373) and by the NSF (grant DMI-0113295).

REFERENCES

1. Gurson, A. L., 1977, Continuum theory of ductile rupture by void nucleation and growth: Part 1 - Yield criteria and flow rules for a porous ductile media, *J. Engr. Mat. Techn.*, Vol. 99, pp. 2–15.
2. Picart, P., Piechel, G., Oudin, J., 1997, Damage influence in the finite element computations for large strains elasto-plastic mechanical structures, In: M. Predeleanu, P. Gilormini (Eds.), *Advanced Methods in Materials Processing Defects, Studies in Applied Mechanics*, Vol. 45, pp. 175–184.
3. Picart, P., Ghouati, O., Gelin, J. C., 1998, Optimization of metal forming process parameters using damage minimization, *J. of Materials Processing Technology*, Vol. 80-81, pp. 597-601.
4. Chung, S. H., Lee, J. H., Chung, H. S., Hwang, S. M., 2000, Process optimal design in non-steady forming of porous metals by the finite element method, *Int. J. of Mechanical Sciences*, Vol. 42, pp. 965–990.
5. Srikanth, A. and Zabarar, N., 1999, A computational model for the finite element analysis of thermoplasticity with ductile damage at finite strains, *Int. J. Numer. Methods Engrg.*, Vol. 45, pp. 1569–1605.
6. Badrinarayanan, S. and Zabarar, N., 1996, A sensitivity analysis for the optimal design of metal forming processes, *Comput. Methods Appl. Mech. Engrg.*, Vol. 129, pp. 319–348.
7. Srikanth, A. and Zabarar, N., 2000, Shape optimization and preform design in metal forming processes, *Comput. Methods Appl. Mech. Engrg.*, Vol. 190, pp. 1859–1901.
8. Ganapathysubramanian, S. and Zabarar, N., 2002, A continuum sensitivity method for finite thermo-inelastic deformations with applications to the design of hot forming processes, *Int. J. Numer. Methods Engrg.*, in press.
9. Zabarar, N., Srikanth, A., Bao, Y., Frazier, W. G., 2000, A continuum Lagrangian sensitivity analysis for metal forming processes with application to die design problems, *Int. J. Numer. Methods Engrg.*, Vol. 48, pp. 679–720.
10. Zavaliangos, A. and Anand, L., 1992, Thermal aspects of shear localization in microporous viscoplastic solids, *Int. J. Numer. Methods Engrg.*, Vol. 33, pp. 595–634.
11. Budiansky, B., 1970, Thermal and thermoelastic properties of isotropic composites, *J. of Composite Materials*, Vol. 4, pp. 286–295.
12. Tvergaard, V. and Needleman, A., 1991, Elastic-viscoplastic analysis of ductile fracture. In: D. Besdo and E. Stein (Eds.), *Finite Inelastic Deformations - Theory and Applications*, IUTAM Symposium - Hannover/Germany, pp. 3–14.
13. Weber, G. and Anand, L., 1990, Finite deformation constitutive equations and a time integration procedure for isotropic, hyperelastic-viscoplastic solids, *Comput. Methods Appl. Mech. Engrg.*, Vol. 79, pp. 173–202.
14. Anand, L., 1985, Constitutive equations for hot working of metals, *Int. J. of Plasticity*, Vol. 1, pp. 213–231.